JOC Article

Photochemistry of 1,2,4-Oxadiazoles. A DFT Study on Photoinduced Competitive Rearrangements of 3-Amino- and 3-*N*-Methylamino-5-perfluoroalkyl-1,2,4-oxadiazoles

Andrea Pace,*,† Silvestre Buscemi,† Nicolò Vivona,† Arturo Silvestri,‡ and Giampaolo Barone*,‡

Dipartimento di Chimica Organica "E. Paternò"and Dipartimento di Chimica Inorganica e Analitica "S. Cannizzaro", Università degli Studi di Palermo, Viale delle Scienze, Parco d'Orleans II, Edificio 17, I-90128 Palermo, Italy

pace@unipa.it; gbarone@unipa.it

Received December 14, 2005

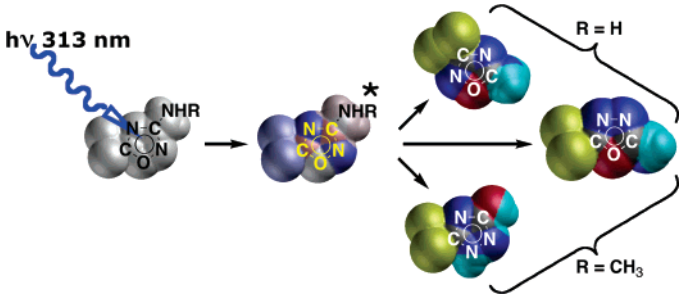

The photoinduced competitive rearrangements of 5-perfluoroalkyl-3-amino(*N*-alkylamino)-1,2,4-oxadiazoles have been investigated by DFT calculations and UV−vis spectroscopy. The observed product selectivity depends on the number of hydrogen atoms present in the amino moiety and involves two or three possible routes: (i) ring contraction−ring expansion (RCRE), (ii) internal-cyclization isomerization (ICI), or (iii) C(3)−N(2) migration−nucleophilic attack−cyclization (MNAC). UV absorption and fluorescence spectra of the reactants, and vertical excitation energy values, calculated by time dependent DFT, support the involvement of a neutral singlet excited state in the photoexcitation process. The values of the standard free energy of the most stable prototropic tautomers of reactant, products, proposed reaction intermediates, and deprotonated anionic transition states allowed us to rationalize the competition among the three rearrangements, in agreement with chemical trapping experiments, in terms of: (i) the evolution of the excited state toward three stable ground-state intermediates, (ii) tautomeric and deprotonation equilibria occurring in methanol solution for each intermediate, and (iii) relative stabilization of intermediates and transition states in the thermally driven section of the reaction.

Introduction

The 1,2,4-oxadiazole (**I**, Chart 1) is an important heterocyclic system whose chemistry has been the object of several reviews and whose applications range from pharmaceuticals to materials science. The 1,2,4-oxadiazole ring is in fact a hydrolysis-resisting bioisoster for amides or esters,[1] and some of its derivatives showed analgesic, antiinflammatory, and antirhinoviral[1a] properties and have also been used as agonists (e.g., for muscarinic[1b,2] and 5-hydroxytryptamine[3]) or antagonists (e.g., for angiotensin[4]) for different receptors. Other useful applications, many of which have been patented, include plant protection,[5] use as liquid crystalline mesophases,[6] dyeing or printing with 1,2,4-oxadiazole azo dyes,[7] and use as constituents

* To whom correspondence should be addressed.
† Dipartimento di Chimica Organica "E. Paternò". Fax +39091596825.
‡ Dipartimento di Chimica Inorganica e Analitica "S. Cannizzaro". Fax +39091427584.

(1) (a) Diana, G. D.; Volkots, D. L.; Nitz, T. J.; Bailey, T. R.; Long, M. A.; Vescio, N.; Aldous, S.; Pevear, D. C.; Dutko, F. J. *J. Med. Chem.* **1994**, *37*, 2421−2436. (b) Saunders, J.; Cassidy, M.; Freedman, S. B.; Harley, E. A.; Iversen, L. L.; Kneen, C.; MacLeod, A. M.; Merchant, K. J.; Snow, R. J.; Baker, R. *J. Med. Chem.* **1990**, *33*, 1128−1138. (c) Borzilleri, R. M.; Zheng, X.; Qian, L.; Ellis, C.; Cai, Z.-wei; Wautlet, B. S.; Mortillo, S.; Jeyaseelan, Sr., R.; Kukral, D. W.; Fura, A.; Kamath, A.; Vyas, V.; Tokarski, J. S.; Barrish, J. C.; Hunt, J. T.; Lombardo, L. J.; Fargnoli, J.; Bhide, R. S. *J. Med. Chem.* **2005**, *48*, 3991−4008. (d) Bokach, N. A.; Khripoun, A. V.; Kukushkin, V. Yu.; Haukka, M.; Pombeiro, A. J. L. *Inorg. Chem.* **2003**, *42*, 896−903.

10.1021/jo0525736 CCC: $33.50
Published on Web 03/02/2006

CHART 1. 1,2,4-Oxadiazole and Its Proposed First-Formed Photolytic Intermediates

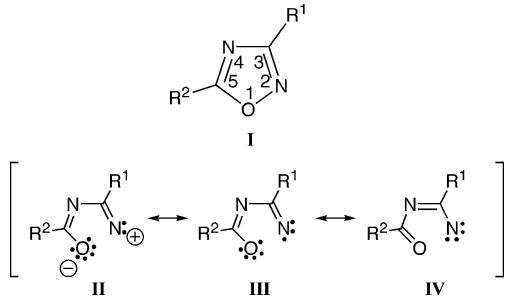

of fluorescent whiteners.[8] These applications represent an important motivation for the study of the synthesis and reactivity of oxadiazole derivatives.

Among five-membered heterocycles, the 1,2,4-oxadiazole presents a high tendency to rearrange into other, more stable, heterocyclic systems.[9−20] This reactivity, which can be either thermally or photochemically induced, depends on several factors such as (i) the presence of a labile O−N bond,[9] (ii) the low aromaticity,[21] (iii) the eventual presence of a participating side-chain at C(3), which may lead to the Boulton−Katritzky rearrangements (BKR),[10,11] (iv) the electrophilic character of N(2) which stems from the ability of the oxygen to act as a good internal leaving group,[11] and (v) the electrophilic character of C(5) induced by the presence of electron-withdrawing substituents.[12]

Strictly referring to photochemical processes, several patterns can be envisaged where a common primary photoprocess involves the cleavage of the O−N bond which supposedly generates an open-chain intermediate with either a zwitterionic (**II**), diradical (**III**), or nitrene-like (**IV**) character (Chart 1), which will then produce the final product, depending on the nature and position of substituents as well as on the presence of a reagent in the photoreaction medium.[9,13]

In this context, besides our historical interest for the oxadiazole heterocycle, we recently looked at the chemistry of fluorinated oxadiazole derivatives and pointed out that the presence of a perfluoroalkyl group strongly affects their chemical and photochemical behavior.[14,15] For instance, 3-amino- and 3-*N*-methylamino-5-perfluoroalkyl-1,2,4-oxadiazoles, irradiated at $\lambda = 313$ nm, showed a marked photoreactivity compared with the nonfluorinated analogues.[15] Their reactivity has been rationalized on the basis of the three pathways illustrated in Scheme 1.[15,18−20] Although some of the routes have also been observed with different substituents at C(5), in the present paper we have chosen to study the reactivity of 5-perfluoroalkyl derivatives since for these substrates all of the routes illustrated in Scheme 1 have been experimentally observed.

Among the most common photochemical processes observed for fluorinated as well as for nonfluorinated 1,2,4-oxadiazoles are (i) solvolysis[16] and (ii) reduction,[17] which lead to open-chain products, (iii) the ring contraction−ring expansion (RCRE) route[15,18] (pathway 1 in Scheme 1), (iv) the Internal-cyclization isomerization (ICI) route[15,19] (Pathway 2 in Scheme 1), and (v) the C(3)−N(2) migration−nucleophilic attack−cyclization (MNAC) route[20] (pathway 3 in Scheme 1).

The RCRE route is observed for both amino and *N*-alkylamino substrates **1a** and **1b** irradiated at 313 nm and in the presence of triethylamine (TEA). The first-formed photolytic species may rearrange into a diazirine intermediate **2**[22] (in analogy with the well-known isoxazole to oxazole rearrangement),[22b−d] which undergoes an intramolecular nucleophilic attack of the carbonyl oxygen onto the C(3) of the diazirine producing 1,3,4-oxadiazole **3**. It is noteworthy that in the 1,2,4-oxadiazole series (fluorinated or not), this process has been observed in solution only in protic solvents (for instance, MeOH)

(2) Macor, J. E.; Ordway, T.; Smith, R. L.; Verhoest, P. R.; Mack, R. A. *J. Org. Chem.* **1996**, *61*, 3228−3229.

(3) (a) Gur, E.; Dremencov, E.; Lerer, B.; Newman, M. E. *Eur. J. Pharmacol.* **2001**, *411*, 115−122. (b) Watson, J.; Selkirk, J. V.; Brown, A. M. *J. Biomol. Screening* **1998**, *3*, 101−105. (c) Pauwels, P. J.; Wurch, T.; Palmier, C.; Colpaert, F. C. *Br. J. Pharmacol.* **1998**, *123*, 51−62.

(4) Naka, T.; Kubo, K. *Curr. Pharm. Des.* **1999**, *5*, 453−472.

(5) (a) Hagen, H.; Becke, F. Ger. Offen. DE 2,060,082, 1972; *Chem. Abstr.* **1972**, *77*, 88511. (b) Hagen, H.; Becke, F.; Niemeyer, J. Ger. Offen. DE 2,016,692, 1971; *Chem. Abstr.* **1972**, *76*, 25299.

(6) Torgova, S. I.; Karamysheva, L. A.; Geivandova, T. A.; Strigazzi, A. *Mol. Cryst. Liq. Cryst. Sci. Technol., Sect. A: Mol. Cryst. Liq. Cryst.* **2001**, *365*, 1055−1062.

(7) (a) Zamponi, A.; Patsch, M.; Hagen, H.; Walther, B.-P. Ger. Offen. DE 19,640,189, 1998; *Chem. Abstr.* **1998**, *128*, 271684. (b) Lamm, G.; Reichelt, H.; Wiesenfeldt, M. Ger. Offen. DE 19,548,785, 1997; *Chem. Abstr.* **1997**, *127*, 110290. Fuerstenwerth, H. Ger. Offen. DE 3,344,294, 1985; *Chem. Abstr.* **1985**, *103*, 215152.

(8) (a) Prossel, G.; Erckel, R.; Schinzel, E.; Guenther, D.; Roesch, G. Ger. Offen. DE 2,748,660, 1978; *Chem. Abstr.* **1978**, *89*, 112427. (b) Schlaepfer, H. Ger. Offen. DE 2,712,409, 1977; *Chem. Abstr.* **1978**, *88*, 51973. (c) Siegrist, A. E.; Kormany, G.; Kabas, G. *Helv. Chim. Acta* **1976**, *59*, 2469−2491. (d) Domerque, A. Ger. Offen. DE 2,503,439, 1975; *Chem. Abstr.* **1975**, *83*, 165830.

(9) Pace, A.; Pibiri, I.; Buscemi, S.; Vivona N. *Heterocycles* **2004**, *63* (11), 2627−2648 and references therein.

(10) (a) Boulton, A. J.; Katritzky, A. R.; Hamid, A. M. *J. Chem. Soc. C* **1967**, 2005−2007. (b) Afridi, A. S.; Katritzky, A. R.; Ramsden, C. A. *J. Chem. Soc., Perkin Trans. 1* **1976**, 315−320. (c) Ruccia, M.; Vivona, N.; Spinelli, D. *Adv. Heterocycl. Chem.* **1981**, *29*, 141−169. (d) L'abbé, G. *J. Heterocycl. Chem.* **1984**, *21*, 627−638. (e) Vivona, N.; Buscemi, S.; Frenna, V.; Cusmano, G. *Adv. Heterocycl. Chem.* **1993**, *56*, 49−154.

(11) For mechanistic studies on azole-to-azole interconversion reactions of the Boulton−Katritzky type, see: Cosimelli, B.; Guernelli, S.; Spinelli, D.; Buscemi, S.; Frenna, V.; Macaluso, G. *J. Org. Chem.* **2001**, *66*, 6124−6129 and references therein.

(12) (a) Buscemi, S.; Pace, A.; Palumbo Piccionello, A.; Macaluso, G.; Vivona N.; Spinelli, D.; Giorgi G. *J. Org. Chem.* **2005**, *70*, 3288−3291. (b) Buscemi, S.; Pace, A.; Pibiri, I.; Vivona, N.; Spinelli, D. *J. Org. Chem.* **2003**, *68*, 605−608. (c) Buscemi, S.; Pace, A.; Pibiri, I.; Vivona, N.; Lanza, C. Z.; Spinelli, D. *Eur. J. Org. Chem.* **2004**, 974−980.

(13) (a) Vivona, N.; Buscemi, S. *Heterocycles* **1995**, *41*, 2095−2116 and references therein. (b) Vivona, N.; Buscemi, S.; Caronna, T. *J. Org. Chem.* **1996**, *61*, 8397−8401. (c) Vivona, N.; Buscemi, S.; Asta, S.; Caronna, T. *Tetrahedron* **1997**, *53*, 12629−12636.

(14) Buscemi, S.; Pace A.; Vivona, N. *Tetrahedron Lett.* **2000**, *41*, 7977−7981

(15) Buscemi, S.; Pace A.; Pibiri, I.; Vivona, N. *J. Fluorine Chem.* **2004**, *125*, 165−173.

(16) (a) Newman, H. *Tetrahedron Lett.* **1968**, 2421−2424. (b) Buscemi, S.; Cicero, M. G.; Vivona, N.; Caronna, T. *J. Heterocycl. Chem.* **1988**, *25*, 931−935.

(17) (a) Newman, H. *Tetrahedron Lett.* **1968**, 2417−2420. (b) Buscemi, S.; Vivona, N.; Caronna, T. *J. Org. Chem.* **1996**, *61*, 8397−8401. (c) Vivona, N.; Buscemi, S.; Asta, S.; Caronna, T. *Tetrahedron* **1997**, *53*, 12629−12636.

(18) (a) Buscemi, S.; Cicero, M. G.; Vivona, N.; Caronna, T. *J. Chem. Soc., Perkin Trans. 1* **1988**, 1313−1315. (b) Buscemi, S.; Cicero, M. G.; Vivona, N.; Caronna, T. *J. Heterocycl. Chem.* **1988**, *25*, 931−935. (c) Buscemi, S.; Pace A.; Vivona, N.; Caronna, T. *J. Heterocycl. Chem.* **2001**, *38*, 777−780.

(19) (a) Buscemi, S.; Pace A.; Pibiri, I.; and Vivona, N. *J. Org. Chem.* **2002**, *67*, 6253−6255. (b) Buscemi, S.; D'Auria, M.; Pace A.; Pibiri, I.; and Vivona, N. *Tetrahedron* **2004**, *60*, 3243−3249

(20) (a) Pace A.; Pibiri, I.; Buscemi, S.; Vivona, N.; Malpezzi, L. *J. Org. Chem.* **2004**, *69*, 4108−4115. (b) Pace A.; Buscemi, S.; Vivona, N. *J. Org. Chem.* **2005**, *70*, 2322−2324.

(21) In the class of five-membered heterocyclic systems, 1,2,4-oxadiazoles are among the least aromatic with an index of aromaticity $I_5 = 39$ or $I_A = 48$. (a) Bird, C. V. *Tetrahedron* **1985**, *41*, 1409−1414. (b) Bird, C. V. *Tetrahedron* **1992**, *48*, 335−340.

SCHEME 1. Photoinduced Ring-rearrangements of 3-Amino (1a) and 3-*N*-Alkylamino-5-perfluoroalkyl-1,2,4-oxadiazoles (1b) in MeOH and in the Presence of a Base

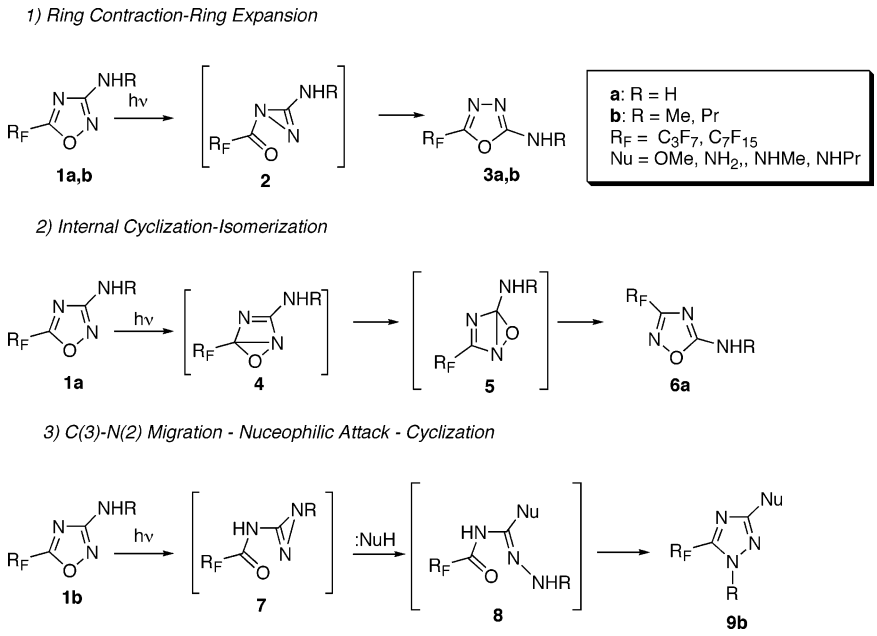

and appears to be restricted to 1,2,4-oxadiazoles bearing an XH group (such as OH, NH_2, or NHR) on the C(3).[18,23]

The ICI route, historically explained through the formation of bicyclic species such as **4** and **5**, is observed (in competition with the RCRE route) only for the 3-amino derivatives **1a** and only in the presence of a base.[20,24] Surprisingly, such a reactivity is completely absent in the case of *N*-alkylamino derivatives **1b**, all other experimental conditions being fixed. Since the electronic substituent effect of an amino or a methylamino group is similar, it seems unlikely that such a small difference may cause this pathway to shut down. A more likely explanation could imply that both NH_2 hydrogen are involved in the reaction pathway.

Finally, a MNAC rearrangement, involving a C(3)−N(2) susbtituent shift, followed by nucleophilic attack and subsequent cyclization, has been observed (in competition with the RCRE route) only for 3-*N*-alkylamino derivatives **1b**.[20a] Here, the exocyclic nitrogen either migrates to N(2) or behaves as an internal nucleophile to give an *exocyclic* diazirine intermediate **7**[25] which will undergo a nucleophilic attack to give intermediate **8**, which will develop into the final 1-alkyl-1,2,4-triazole **9b**.

Despite the sound amount of reactions explored by our and other groups, the proposed intermediate species (in square brackets in Scheme 1) have never been isolated. As a consequence, for the 1,2,4-oxadiazole system, the three reaction mechanisms above have been drawn on the basis of (i) the structure of the final products, (ii) comparison with proved mechanisms for similar reactions of other five-membered heterocycles (i.e., the isoxazole or the oxazole rings),[22b−d] and (iii) qualitative information on the influence of experimental conditions on the overall outcome of the reaction.

In several cases, heterocyclic rearrangements have also been rationalized by the support of quantum chemical methods.[19b,26] In a recent study on the ring-photoisomerization of some 3-amino-5-alkyl(aryl)-1,2,4-oxadiazoles,[19b] we based our approach on the hypothesis that the singlet excited state of a heterocyclic molecule decays either into the corresponding Dewar isomer leading to ICI isomerization or into the triplet excited state which generates a biradical intermediate leading to RCRE products. Computational findings were in agreement with experimental results, which were explained on the basis of the energies of the first-formed photolytic intermediates. Moreover, calculations performed on anionic deprotonated species supported the intervention of a base catalysis in the reaction pathway.

In the present case study, depending on nitrogen substituent R (H or Me), only two out of the three possible reaction routes are observed (see Scheme 1). To justify this reactivity, we performed a combined experimental and computational study aimed to reveal the nature of the involved excited states, the existence and stability of proposed intermediates, and the involvement of acid−base or prototropic tautomeric equilibria among intermediates. The experimental observations were based on UV−vis absorption and emission spectra and chemical trapping experiments. The electronic transitions occurring in the UV−vis range experimentally investigated were interpreted by the support of time-dependent (TD) DFT calculations performed on the isolated **10a,b** compounds. Finally, we have described the thermochemistry of the reaction, i.e., the post-photoexcitation development of intermediates. DFT calculations, including solvent effects, have been performed on the neutral and deprotonated anionic forms of 3-amino- and 3-*N*-methylamino-5-trifluoromethyl-1,2,4-oxadiazoles **10a,b** (as model structures for **1a,b**)[27] as well as on the related products and on the

(22) (a) Some diazirine intermediates have been well documented in the photoreaction of sydnones, see: Padwa, A. In *Rearrangements in Ground and Excited States*; De Mayo, P., Ed.; Academic Press: New York, 1980; Vol III. (b) 1-Azirine intermediates have been isolated in the photorearrangement of isoxazoles: Ullman, E. F.; Singh, B. *J. Org. Chem.* **1966**, *31*, 1844−1845. (c) Ullman, E. F.; Singh, B. *J. Org. Chem.* **1967**, *32*, 6911−6916. (d) Singh, B.; Zweig, A.; Gallivan, J. B. *J. Am. Chem. Soc.* **1972**, *94*, 1199−1206. (e) 2-Diazirines are intrinsically instable due to their antiaromatic character. Heine, H. W. in *Heterocyclic Compounds*; Hassner, A., Ed.; John Wiley: New York, 1983; Vol. 42, Part 2, pp 549−628.

(23) Exceptions to these requirements have been reported for irradiations in heterogeneous constrained media.[20b]

(24) The ICI route in the 1,2,4-oxadiazole series has been observed also for 5-alkyl-3-amino derivatives.[19]

SCHEME 2. Standard Free Energy Values, Calculated in MeOH, along the Three Reaction Routes[a]

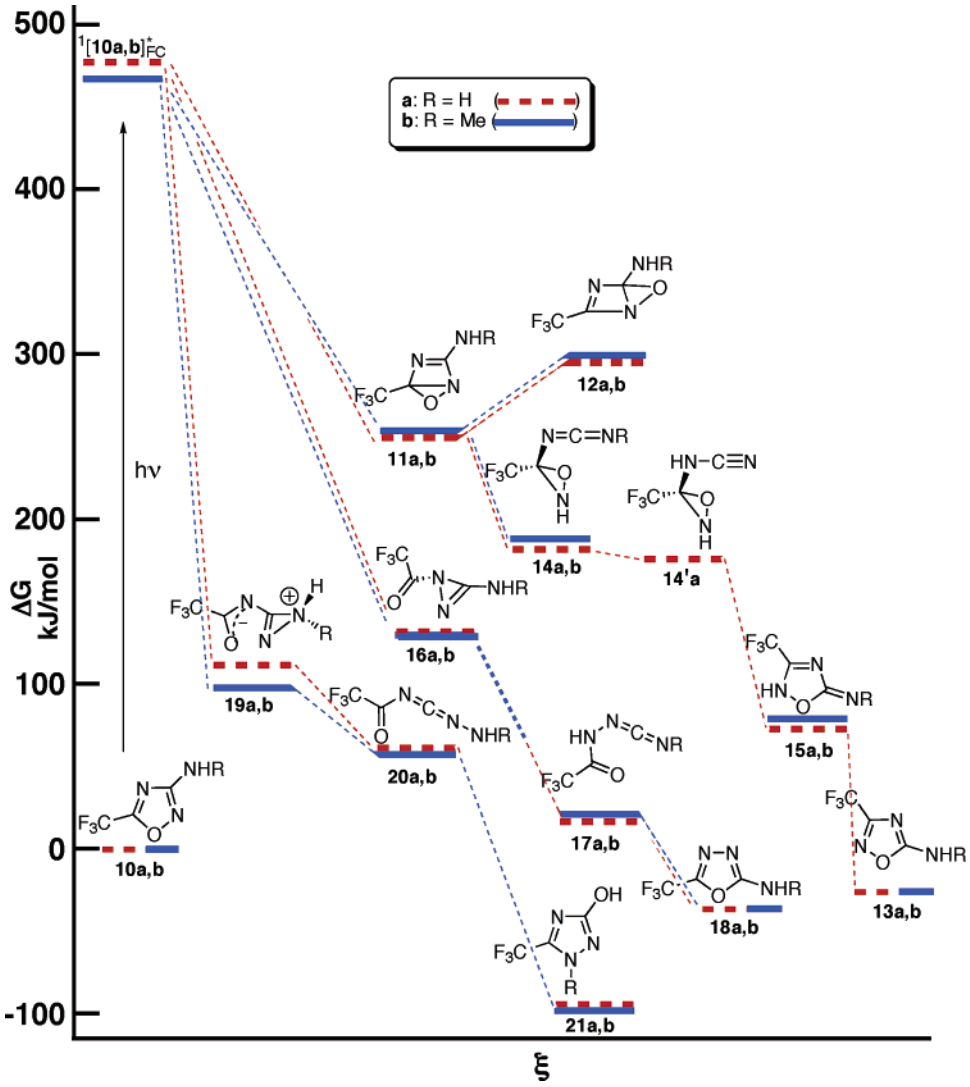

[a] The energy values of ^{1}[**10a,b**]*$_{FC}$ were experimentally obtained from the UV absorption maxima.

intermediates proposed along the reaction coordinate (see compounds **11**−**21a,b** and **11**−**21a,b**$^-$ in Schemes 2 and 3). In particular, compounds **11**, **12**, and **13** are models for **4**, **5**, and **6**, respectively; compounds **16** and **18** are models for **2** and **3**, respectively; compounds **19**, **20**, and **21** are models for **7**, **8**, and **9**, respectively. Furthermore, transition states between the proposed intermediates have been considered in an anionic reaction pathway to rationalize the requirement of a base and of a protic solvent for the occurrence of the observed photo-induced ring rearrangements.

(25) (a) Jones, S. S.; Staiger, D. B.; Chodosh, D. F. *J. Org. Chem.* **1982**, *47*, 1969−1971. (b) Braun, M.; Buchi, G.; Bushey, D. F. *J. Am. Chem. Soc.* **1978**, *100*, 4208−4213.

(26) See, among others: (a) Sampedro, D.; Soldevilla, A.; Rodriguez, M. A.; Campos, P. J.; Olivucci, M. *J. Am. Chem. Soc.* **2005**, *127*, 441−448. (b) Bottoni, A.; Frenna, V.; Lanza, C. Z.; Macaluso, G.; Spinelli, D. *J. Phys. Chem. A* **2004**, *108*, 1731−1740. (c) Tanaka, H.; Matsushita, T.; Nishimoto, K. *J. Am. Chem. Soc.* **1983**, *105*, 1753−1760. (d) Srivastava, R. M.; Faustino, W. M., Brinn, I. M. *J. Mol. Struct.* **2003**, *640*, 49−56.

(27) As a matter of fact, the photoreactivity of the volatile 5-trifluoromethyl derivative **10b**, studied during one-pot prolonged irradiations of 3-trifluoroacetylaminofurazans at 313 nm in MeOH/$MeNH_2$, led to the formation of **18b** and of 1-methyl-3-*N*-methylamino-5-trifluoromethyl-1,2,4-triazole in analogy to that observed for compounds **1b** ($R_F = C_3F_7$, C_7F_{15}).[20a]

Results and Discussion

The present study is based on the hypothesis, supported by experimental findings, that the photoexcitation of **1a,b** gives rise to an excited state, with a weakened O−N bond, which then proceeds to the final products via thermal pathways (i.e., ground-state chemistry of the first-formed intermediates).

To investigate the excitation process, the UV absorption and fluorescence spectra of **1a** and **1b** (R = Me) and **10a,b** have been registered (see Table 1).

The vertical excitation energy values, toward two singlet and two triplet states, of both the neutral and deprotonated substrates in vacuo, have been calculated by the TD-DFT method and reported in Table 2.

The neutral molecular species have been investigated together with their related lowest energy deprotonated forms. The relative standard free energy values of all the studied species, calculated in vacuo and in methanol, are reported in Table 3. For all species, we reported only the most stable tautomers found. To compare the energy values of all the participants to the reaction, the isomeric compounds **21a,b** were chosen to represent the

SCHEME 3. Standard Free Energy Values, Calculated in MeOH, along the Three Reaction Routes[a]

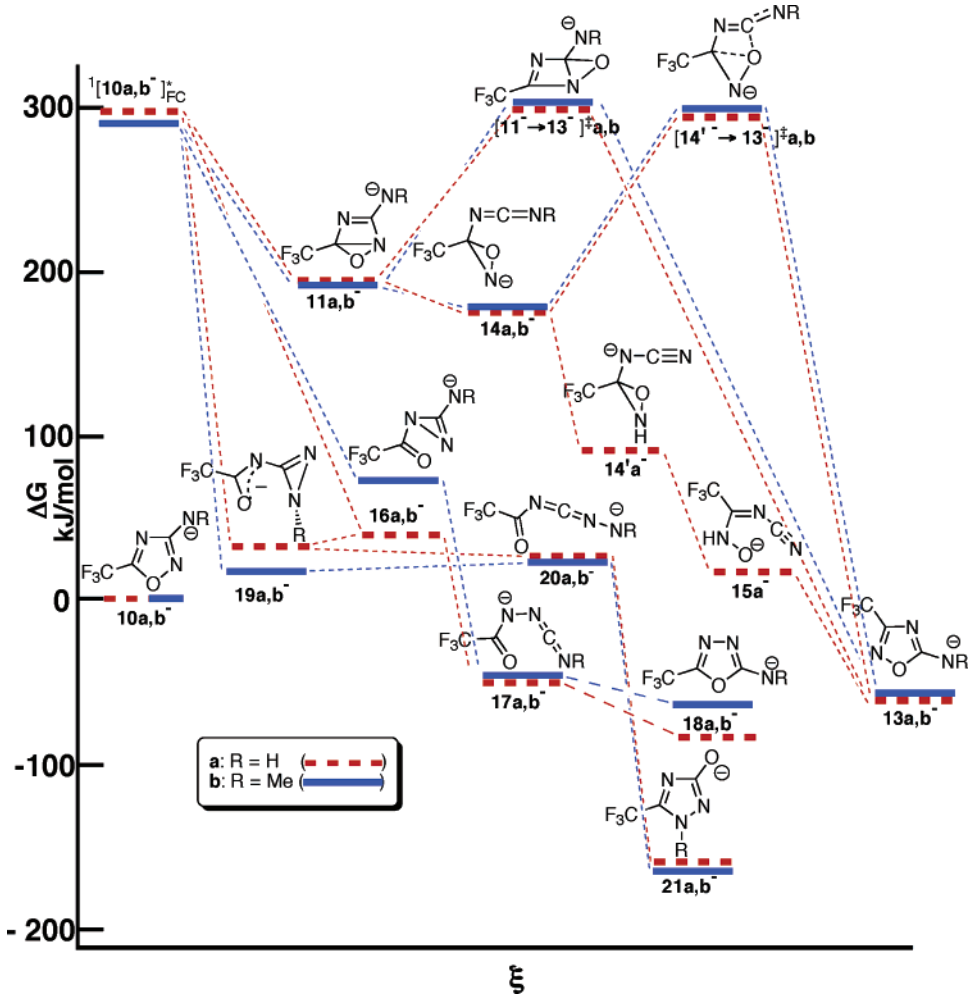

[a] The energy values of $^1[\mathbf{10a,b}^-]^*_{FC}$ have been estimated by TD-DFT calculations in vacuo.

TABLE 1. UV−Vis Absorption (λ_{max} and E Values) and First Singlet Excited-State Energies (E_S) (from Emission Spectra) of 1a,b and 10a,b

	UV absorption[a]		
compd	λ_{max} (nm)	ϵ	E_S (kJ/mol)
10a	251	1200	406
1a ($R_F = C_3F_7$)[b]	257	1200	385
1a ($R_F = C_7F_{15}$)[b]	259	1200	389
1a ($R_F = C_7F_{15}$)	255[c]	1250	
1a ($R_F = C_7F_{15}$)	244[d]	1400	
10b	257	1300	385
1b (R = Me; $R_F = C_3F_7$)	267	1000	342
1b (R = Me; $R_F = C_7F_{15}$)	269	1100	362

[a] In methanol. [b] Data from ref 15. [c] In acetonitrile. [d] In cyclohexane.

TABLE 2. Vertical Excitation Energies of Singlet (S) and Triplet (T) States, Calculated in Vacuo at the TD-DFT Level, for Neutral and Deprotonated Forms of 10a,b

	excitation energy (kJ/mol)			
compd	S_1	S_2	T_1	T_2
10a	488.7	509.9	352.6	480.6
10b	458.1	521.8	342.5	468.5
10a$^-$	297.8	332.5	214.0	325.4
10b$^-$	290.6	299.4	220.4	290.1

1,2,4-triazole products **9**, assuming the hydroxide anion as nucleophilic reagent (not considered in Scheme 1).

Structures and free energy values calculated in methanol solution for the three investigated reaction routes are illustrated in Scheme 2 for neutral and in Scheme 3 for deprotonated anionic species. The reported energy values are referred to the corresponding starting oxadiazoles **10a,b** or **10a,b**$^-$.

The Excitation Process. The absorption data (Table 1) agree with the hypothesis of a $\pi-\pi^*$ electronic transition involved in the photoexcitation. In fact, the large molar extinction coefficient values ($\epsilon \sim 10^3$) of the absorption maxima allow us to exclude a pure n$-\pi^*$ transition, which is usually characterized by an ϵ value ranging between 0.01 and 100.[28] Furthermore, the spectra recorded in different solvents for representative compound **1a** ($R_F = C_7F_{15}$) showed a bathochromic shift of up to 15 nm by increasing the solvent polarity from cyclohexane to methanol (see Figure 1). This trend is typical of a $\pi-\pi^*$ transition and indicates the formation of a polar or charge-separated (zwitterionic) excited state.[28]

Moreover, UV spectra were not affected by the addition of different amounts of triethylamine (TEA), thus excluding the formation of deprotonated species in the ground state under the same conditions used during irradiation.[29]

(28) Turro, N. J. *Modern Molecular Photochemistry*; Benjamin/Cummings: Menlo Park, CA, 1978.

TABLE 3. Standard Free Energy Values (kJ/mol) Relative to Compound 10a,b[a] and 10a,b$^-$,[b] Calculated in Vacuo and in MeOH at 298.15 K

neutral species	in vacuo	in MeOH	deprotonated species	in vacuo	in MeOH
10a	0	0	**10a**$^-$	0	0
10b	0	0	**10b**$^-$	0	0
11a	263.7	249.3	**11a**$^-$	190.0	196.6
11b	265.4	252.1	**11b**$^-$	189.8	195.0
12a	298.3	295.7	**12a**$^-$	*c*	*c*
12b	300.3	298.9	**12b**$^-$	*c*	*c*
13a	−19.9	−29.0	**13a**$^-$	−73.6	−61.7
13b	−20.9	−29.5	**13b**$^-$	−71.1	−57.0
14a	187.2	181.0	**14a**$^-$	181.7	176.9
14b	182.4	186.9	**14b**$^-$	185.8	178.6
14′a[d]	207.9	173.7	**14′a**$^-$ [d]	81.7	90.4
15a	88.8	67.0	**15a**$^-$ [d]	12.4	16.4
15b	90.5	77.4			
16a	148.5	129.1	**16a**$^-$	46.8	40.5
16b	145.9	128.1	**16b**$^-$	58.7	71.7
17a	26.3	16.4	**17a**$^-$	−62.5	−49.9
17b	19.2	20.0	**17b**$^-$	−61.0	−47.8
18a	−25.3	−37.2	**18a**$^-$	−78.3	−85.9
18b	−25.6	−36.9	**18b**$^-$	−74.0	−66.4
19a	153.2	108.9	**19a**$^-$	6.6	31.7
19b	131.3	95.3	**19b**$^-$	−5.2	16.6
20a	69.3	60.3	**20a**$^-$	0.1	24.1
20b	62.6	57.4	**20b**$^-$	−4.1	23.3
21a	−73.5	−94.8	**21a**$^-$	−129.6	−159.4
21b	−87.0	−97.3	**21b**$^-$	−136.7	−165.6

[a] The standard free energy values calculated at the B3LYP/6-31++G(D,P) level are −654.4865 au (for **10a**) and −693.7716 au (for **10b**); the solvation free energy values are −10.07 kcal/mol (for **10a**) and −9.55 kcal/mol (for **10b**). [b] The standard free energy values calculated at B3LYP/6-31++G(D,P) level are −653.9345 au (for **10a**$^-$) and −693.2182 au (for **10b**$^-$); the solvation free energy values are −58.5 kcal/mol (for **10a**$^-$) and −56.8 kcal/mol (for **10b**$^-$). [c] The structures of anionic species **12a,b**$^-$ are not stable after geometry optimization. Incidentally, the structure of the anionic transition states **[11→13]‡a,b**$^-$ is very similar to that of neutral species **12a,b**. [d] This species is not accessible for R = Me since its formation would involve a methyl shift.

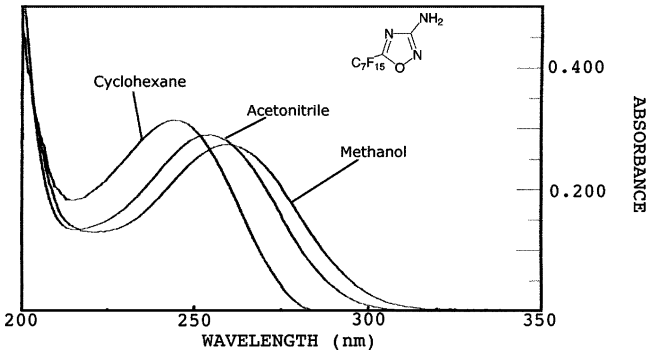

FIGURE 1. UV−vis absorption spectra of **1a** ($R_F = C_7F_{15}$) in the indicated solvent media.

TD-DFT calculations furnished vertical transition energies of 489 and 458 kJ/mol for ^{1}[**10a**]* (S_1) and ^{1}[**10b**]* (S_1), respectively (see Table 2). These energies, which correspond to 245 and 261 nm, respectively, reproduce the bathochromic shift of the 3-methylamino **10b** compared to the 3-amino **10a** derivative, as well as their experimentally observed transition energy difference. The calculated energies of the S_2 levels are of 510 and 522 kJ/mol for ^{1}[**10a**]* (S_2) and ^{1}[**10b**]* (S_2), respectively, and are too high to be reached by irradiation at 313 nm. The calculated oscillator strengths obviously confirm that the singlet−triplet transitions are forbidden. The vertical excitation energies to the first triplet state T_1 are 352 and 342 kJ/mol for ^{3}[**10a**]* and ^{3}[**10b**]*, respectively (see Table 2). The calculated singlet−triplet energy gap ΔE_{S1-T1}, larger than 100 kJ/mol, is typical of a $\pi-\pi^*$ transition.[28] Moreover, such an energy gap would imply a highly unfavorable Franck−Condon factor for an efficient singlet−triplet intersystem crossing.[28] These considerations lead us to consider that the first singlet excited-state S_1 (^{1}[**10a,b**]*) is the common intermediate from which the observed photoreactivity originates.

The TD-DFT analysis showed that the $S_0 \rightarrow S_1$ is a hybrid transition, composed principally by that from the highest occupied to the lowest unoccupied Kohn−Sham molecular orbital (HOMO−LUMO) and, to a lesser extent, by that from the highest occupied to the next lowest unoccupied (HOMO−NLUMO) orbital (see Figure 2). It is noteworthy that the O(1)−N(2) bond is weakened by the π-antibonding character of LUMO and σ-antibonding character of NLUMO. Moreover, in agreement with the observed photoreactivity, the population analysis of the frontier orbitals supports the hypothesis that the N(2) atom increases its electrophilic character in the excited-state S_1. Interestingly, a partially bonding interaction between C(5) and N(2) in the LUMO may justify the evolution of ^{1}[**10a,b**]* into the bicyclic dewar-like structure **11a,b**.

To get an estimate of the relaxed structure of the excited state, we have optimized the geometry of ^{1}[**10a**]* by the configurational interaction singles (CIS) method.[30−32] The resulting structure (see the Supporting Information) has the fluorinated methyl group out of the oxadiazole plane and shows a weakening of the O(1)−N(2) bond, increased by about 0.1 Å with respect to ground state **10a**, in agreement with the analysis above. Moreover, the *exocyclic* nitrogen has a planar geometry at difference with its pyramidal configuration in the ground-state structure.

As far as anionic deprotonated forms are concerned, the $S_0 \rightarrow S_1$ vertical transition energies are 298 and 291 kJ/mol for ^{1}[**10a**$^-$]* and ^{1}[**10b**$^-$]*, respectively. These energies correspond to transitions occurring at 402 and 412 nm and are too much distant from the used irradiation wavelength of 313 nm. In this context, it is worth mentioning that S_1 $\pi-\pi^*$ states often give rise to proton-transfer reactions.[28] Moreover, the σ-antibonding interaction between N and H of the 3-amino (or 3-methylamino) group in the NLUMO suggests that deprotonation reactions would easily occur at the excited-state level. Therefore, in our mechanistic hypothesis, anionic excited states ^{1}[**10a,b**$^-$]* only derive from the deprotonation of neutral excited states ^{1}[**10a,b**]*.

The Development of the Excited State and Reaction Intermediates. Irradiation of **1a** in methanol only[15] (Scheme 4) led to two kinds of open-chain products resulting from two competitive pathways since their formation is also observed at low conversion: the first one (**22**)[15] has been interpreted in terms of solvent trapping of the excited state, or of the first-formed zwitterionic intermediate, by nucleophilic attack on the elec-

(29) It is our opinion that TEA plays only the role of a base and not of an electron-donor reagent since similar results were obtained also using nondonor bases.[18c] See also: Pavlik, J. W.; Tongcharoensirikul, P.; French, K. M. *J. Org. Chem.* **1998**, *63*, 5592−5603.

(30) Foresman, J. B.; Frisch, Æ. *Exploring Chemistry with Electronic Structure Methods*, 2nd ed.; Gaussian, Inc.: Pittsburgh, PA, 1996.

(31) Although it is known that the CIS method is not accurate in the evaluation of the excitation energies, its reliability for obtaining fairly good excited state geometries has been recently reported.[32]

(32) Cramer, C. J. *Essentials of Computational Chemistry*, 2nd ed.; Wiley: New York, 2004.

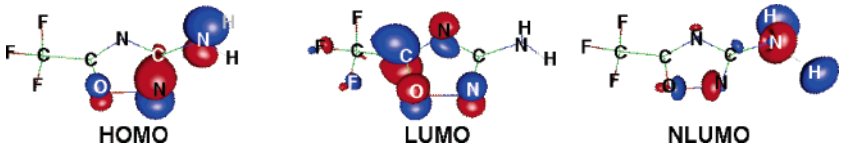

FIGURE 2. Highest occupied, lowest unoccupied, and next lowest unoccupied Kohn−Sham molecular orbitals involved in the $S_0 \rightarrow S_1$ vertical transition of compound **10a**.

SCHEME 4. Irradiations of Compounds 1a,b in Methanol

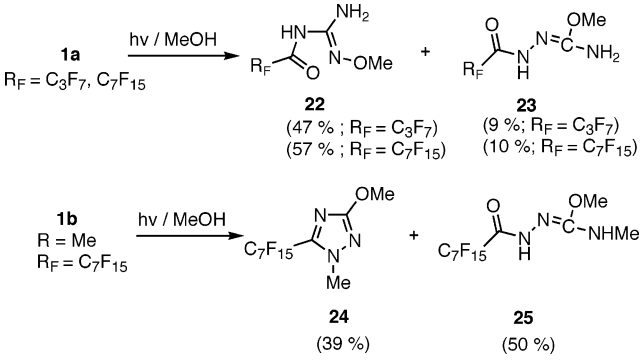

trophilic N(2). The second one (**23**)[15] contains a N(4)−N(2) bond and is explained as the solvent trapping of the diazirine intermediate **2**, suggesting that the nucleophilic attack by the solvent on the C(3) occurs after a ring-contraction step (see Scheme 1, reaction pathway 1). Interestingly, irradiation of **1b** (R = Me; $R_F = C_7F_{15}$) in methanol[20a] (Scheme 4), besides the solvolysis product **25**,[20a] showed the formation of triazole **24**[20a] (MNAC product) where the solvent attacks the C(3) after the migration of the amino group to the N(2).[25a] (See also Scheme 1, reaction pathway 3, and the reaction pathway leading to **21** in Schemes 2 and 3).

The title photoreactions (Scheme 1) have been observed in the presence of a base, and this suggests the involvement of either deprotonated or tautomeric species as key intermediates. Moreover, after irradiations in methanol only, no trace of the regioisomer product **6**, or of its precursors (Scheme 1), were found, thus suggesting that a deprotonation step, followed by an anion route, is fundamental especially for the internal cyclization−isomerization pathway.

By evaluating the difference between the acidic equilibrium constants of **^{1}[10a,b]*** and **10a,b** from the vertical excitation energy of **10a,b**$^-$ and **10a,b** (see Table 2), we estimate that the excited states of our reactant molecules are about 30 orders of magnitude more acidic than the corresponding ground state.[33] Therefore, in a protic solvent such as methanol and in the presence of a base such as TEA acid−base equilibria should be fast enough to occur at the oxadiazole excited-state level before its transformation into subsequent reaction intermediates.

By performing DFT calculations, we have checked that the structures of all the proposed intermediates, evidently not sufficiently stable to be isolated, correspond to energy minima in the ground-state potential energy surface. All of these intermediates (Scheme 2) have lower energies with respect to the Franck−Condon excited state ^{1}[**10a,b**]*$_{FC}$, arising from the vertical transition of **10a,b**. Therefore, all three reaction pathways are photochemically accessible. By looking at the deprotonated anionic forms (Scheme 3), the relative energy order is analogous to that found for the neutral species.

Among the three observed reactions, the MNAC route leads to the most stable product. However, it is clear from the energy diagrams (Schemes 2 and 3 and Table 3) that the three first-formed species follow a different stability order (**19** > **16** > **11**) than the subsequent intermediates (**17** > **20** > **14**). Therefore, the observed product distribution should be the result of thermochemically and/or kinetically favored processes, related to structural properties of the involved species.

We have also analyzed the kinetic pathways of the deprotonated species. This approach is justified also by the fact that in a protic solvent, proton exchanges are very fast and should not be determinant for the overall reaction rate. Energetic levels for transition states are all reported in Table 4 and illustrated in Scheme 5 for the transformations **16** → **17**, **19** → **20**,[25b] and **19** → **16**.

Based on the results of DFT calculations, our mechanistic hypothesis is able to explain: (a) the role of an XH moiety at C(3) for the RCRE route to occur; (b) the absence of an ICI route for the methylamino derivatives **1b**; and (c) the absence of a MNAC route for the amino derivatives **1a**.

(a) The Ring Contraction−Ring Expansion Route. This reaction mechanism has always been proposed to occur through a diazirine-like intermediate which has never been isolated[22] due to its supposedly high reactivity.[22e] Since solvent-trapped products such as **23** and **25** (see Scheme 4) contain a N(2)−N(4) bond, the nucleophilic attack by the solvent at the C(3) has to take place either on the diazirine **16a,b** or on the carbodiimide **17a,b**. The latter is much more stable than the diazirine in both neutral and deprotonated forms (see Schemes 2 and 3 and Table 3). Moreover, the development of diazirine **16** into the carbodiimide **17** through the anion route has a small (for R = Me) or no energy barrier. Finally, the presence of a mobile proton (i.e., of an XH moiety at C3) and of a base in the reaction medium will also facilitate the ring closure of **17** into **18** through its anionic form.

(b) The Internal Cyclization−Isomerization Route. Among byciclic intermediates, the Dewar-like isomer **12** is higher in energy than **11**, and this would exclude its involvement in the ICI route at difference with previous suggestions.[15,19] The analysis of all of its possible tautomeric forms showed that **11a,b** may develop into **14a,b**. This species, only when R = H, may develop into the more stable tautomer **14′a**, leading to the final oxadiazole regioisomer **13** for example through its tautomeric form **15a** (see Schemes 2 and 3).[34] The direct transformation of **11a,b**$^-$ into **13a,b**$^-$ has been also considered. This transformation, however, has an activation barrier of 107 kJ/mol, for **11a**, and of 126 kJ/mol, for **11b**, and passes through a transition state (**[11a,b**$^-$ → **13a,b**$^-$**]**‡ in Table 4 and Scheme 3) which is

(33) Estimated from pK_a - pK_a* = $(\Delta E_{10^*-10} - \Delta E_{10^{*-}-10^-})/2.303RT$. Soltsev, K. M.; Huppert, D.; Agmon, N. *J. Phys. Chem. A* **1998**, *102*, 9599−9606.

(34) One of the reviewers suggested that **14b** might develop into **15b** through a neutral reaction pathway. However, we have calculated that such a process has an activation energy barrier, in methanol, of 125.5 kJ/mol, through a transition state that is higher in energy than **12b**.

TABLE 4. Standard Free Energy Values (kJ/mol) Relative to Compound 10a,b$^-$, Calculated for the Anionic Transition States in Vacuo and in MeOH at 298.15 K, and Activation Barriers $\Delta G^{\ddagger}$ (kJ/mol) in MeOH

transition states R = H	in vacuo	in MeOH	$\Delta G^{\ddagger}$	transition states R = Me	in vacuo	in MeOH	$\Delta G^{\ddagger}$
[**11a**$^-$ → **13a**$^-$]‡	305.4	303.6	107.0	[**11b**$^-$ → **13b**$^-$]‡	313.7	321.4	126.4
[**11a**$^-$ → **14a**$^-$]‡	242.2	246.3	49.7	[**11b**$^-$ → **14b**$^-$]‡	247.7	251.2	56.3
[**14a**$^-$ → **13a**$^-$]‡	300.7	294.3	117.4	[**14b**$^-$ → **13b**$^-$]‡	302.0	302.3	123.7
[**14′a**$^-$ → **15a**$^-$]‡	145.4	153.5	63.1	*a*			
[**16a**$^-$ → **17a**$^-$]‡	46.5	40.2	0	[**16b**$^-$ → **17b**$^-$]‡	70.8	80.3	8.6
[**17a**$^-$ → **18a**$^-$]‡	−25.5	−34.4	15.5	[**17b**$^-$ → **18b**$^-$]‡	−21.8	−12.5	35.3
[**19a**$^-$ → **16a**$^-$]‡	128.8	136.7	105.0	[**19b**$^-$ → **16b**$^-$]‡	125.1	146.0	129.4
[**19a**$^-$ → **20a**$^-$]‡	133.9	144.9	113.2	[**19b**$^-$ → **20b**$^-$]‡	116.5	135.0	118.4

[a] The corresponding transformation is not possible for methyl derivatives.

SCHEME 5. Anionic Kinetic Pathways for the Transformation of Intermediate 16a,b$^-$ into 17a,b$^-$ and of 19a,b$^-$ into 20a,b$^-$ or 16a,b$^-$ (Energies Are Referred to 10a,b$^-$)

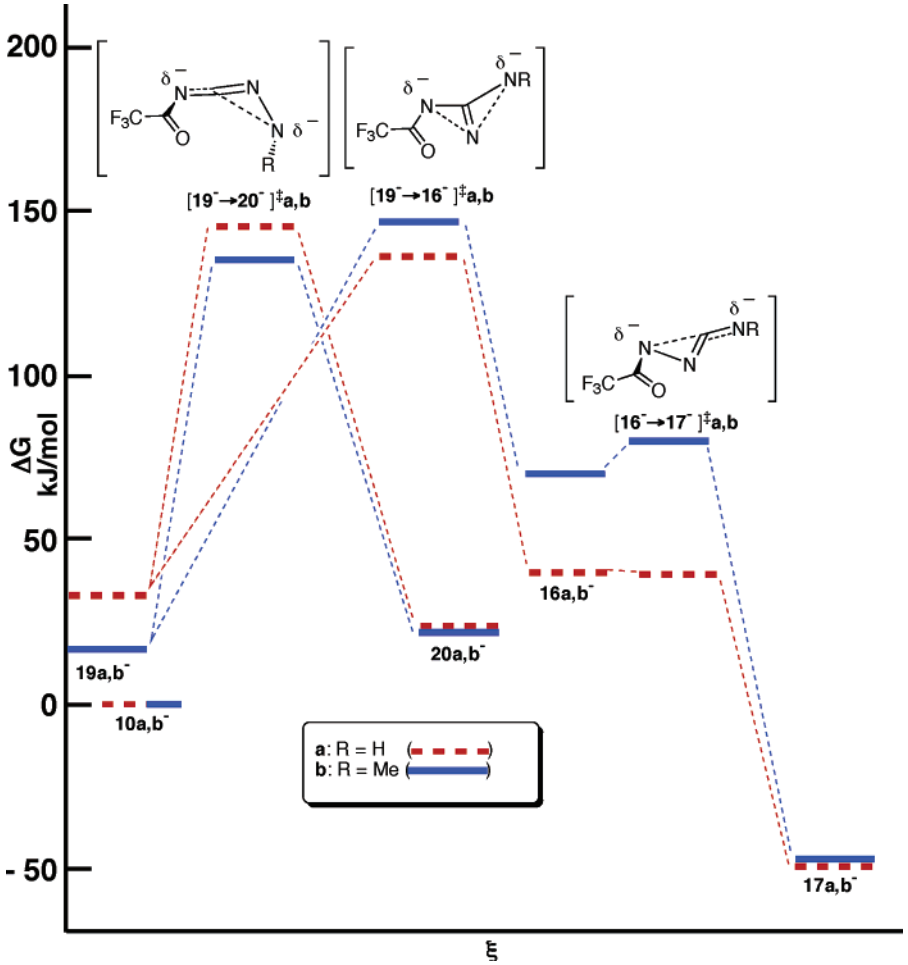

very high in energy and has a geometry very close to the Dewar-like structure **12**. On the other hand, **11a,b**$^-$ may develop into **14a,b**$^-$ through an activation barrier of only 49.7 kJ/mol for **11a** and 56.3 kJ/mol for **11b** (see Table 4). However, the transformation of **14a,b**$^-$ into **13a,b**$^-$ has an activation barrier of 117.4 kJ/mol for **14a** and of 123.7 kJ/mol for **14b**. Alternatively, the development of **14a**$^-$ into the more stable tautomeric anion **14′a**$^-$ can easily occur in a protic solvent. Finally, **14′a**$^-$ develops into **15a**$^-$ by crossing an activation barrier of 63 kJ/mol. These results strongly support the involvement of **14′a**$^-$ in the reaction and well explain why such reactivity is not observed for methylamino derivatives. In fact, in the neutral route (for the formation of **14′a**, see Scheme 2) but principally in the base catalyzed anion route (for the formation of the more stable anionic form **14′a**$^-$, see Scheme 3) both hydrogen atoms of the amino group are involved. Therefore this route is precluded when an alkyl substituent is present on the amino nitrogen.

(c) The C(3)−N(2) Migration−Nucleophilic Attack−Cyclization Route. The free energy values calculated for the intermediates do not show any main difference between amino and methylamino derivatives (see Schemes 2 and 3 and Table 3). Therefore, the occurrence of this reaction should be allowed for both substrates. However, the MNAC route has been observed only for *N*-alkylamino derivatives **1b**. A possible explanation has been obtained by analyzing the related anionic kinetic pathways. In fact, the anionic species **19a,b**$^-$ can be either directly formed from the excited anionic ^{1}[**10a,b**$^-$]* or

SCHEME 6

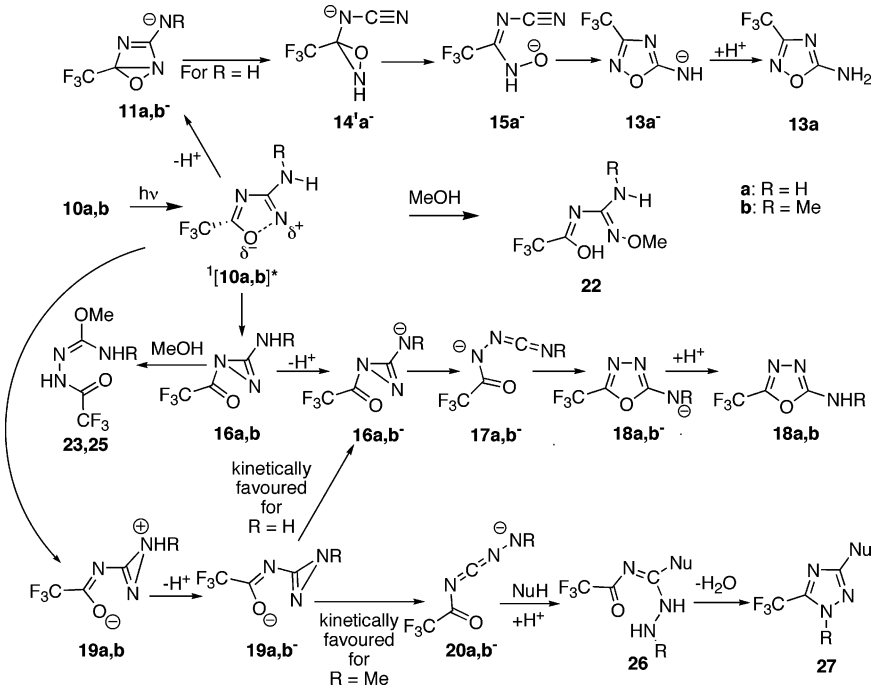

derived from deprotonation of the ammonium-like moiety of **19**. Furthermore, an interconversion between **16**$^-$ and **19**$^-$ may still in principle occur, since they essentially differ only about the N(2)−$N_{exocyclic}$ and N(2)−N(4) distances (see Schemes 3 and 5). Interestingly, when R = H the transformation **19a**$^-$ → **16a**$^-$ → **17a**$^-$ is kinetically favored versus the development of **19a**$^-$ → **20a**$^-$ (Scheme 5), although **20a** is thermodynamically favored. This would explain why in the case of amino derivatives the route leading to triazole is not observed. For methylamino derivatives (R = Me; Scheme 5) instead, the development of **19b**$^-$ → **20b**$^-$ is the preferred route and leads to the formation of 1-methyl-5-perfluoroalkyl-1,2,4-triazoles.

Conclusions

For the title reactions a series of proposed species in both neutral and deprotonated forms, their corresponding most stable prototropic tautomers, and the transition states between anionic intermediates have been studied by DFT calculations. The obtained results pointed out that in the photoinduced rearrangements of 3-amino-5-perfluoroalkyl-1,2,4-oxadiazoles the number of hydrogen atoms present in the amino moiety is fundamental for product selectivity.

Both experimental and theoretical results allowed us to rationalize the thermally driven section of the reaction, in terms of (i) tautomeric and deprotonation equilibria, which in some cases are not accessible depending on the number of hydrogens, and (ii) the relative stabilization of intermediates and transition states. The involvement of a neutral singlet excited state in the photochemical excitation mechanism was inferred on the basis of UV absorption and fluorescence spectra and of TD-DFT calculations.

The main conclusions of this study can be summarized as follows (Scheme 6):

(i) For the ring-degenerate rearrangement through the internal cyclization−isomerization route, both hydrogen atoms of the NH_2 are involved in the crucial steps of this reaction.

(ii) For the photochemical rearrangement of 1,2,4- to 1,3,4-oxadiazoles at least one hydrogen is abstracted or transferred during the formation of the carbodiimide intermediate **17**$^-$ or **17**.

(iii) Finally, in the MNAC route the exocyclic diazirine **19**, which can be easily deprotonated, can develop into **16**$^-$ when R = H or into **20**$^-$ when R = Me following the kinetically favored pattern.

Experimental Section

Computational Details. The molecular and anionic species considered here, shown in Schemes 2 and 3, were selected as the lowest energy conformations among the most stable tautomers found for each isomer. Their geometry was fully optimized by using the hybrid DFT B3LYP method[35] with the 6-31++G(D,P) basis set.[36] Their Cartesian coordinates are available in the Supporting Information.

Transition-state structures were found by the synchronous transit-guided quasi-Newton method.[37] Vibration frequency calculations, within the harmonic approximation, were performed to confirm whether each obtained geometry represented a transition state or a minimum in the potential energy surface. All of the minimum energy structures presented only real vibrational frequencies, whereas all of the transition state structures found were first-order saddle points.

To take into account the relative stabilization of intermediates, the standard free energies, at 298.15 K, of the considered species have been evaluated by vibrational frequency calculations of the in vacuo species. Their free energy in methanol solution was evaluated by adding the solvation free energy to the free energy of the species in vacuo.[32] The solvation free energy in methanol was

(35) Becke, A. D. *J. Chem. Phys.* **1993**, *98*, 5648−5652.

(36) (a) Hehre, W. J.; Ditchfield, R.; Pople, J. A. *J. Chem. Phys.* **1972**, *56*, 2257−2261. (b) Clark, T.; Chandrasekhar, J.; Schleyer, P. V. R. *J. Comput. Chem.* **1983**, *4*, 294−301. (c) Krishnam, R.; Binkley, J. S.; Seeger, R.; Pople, J. A. *J. Chem. Phys.* **1980**, *72*, 650−654. (d) Gill, P. M. W.; Johnson, B. G.; Pople, J. A.; Frisch, M. J. *Chem. Phys. Lett.* **1992**, *197*, 499−505.

(37) Peng, C.; Schlegel, H. B. *Isr. J. Chem.* **1994**, *33*, 449−454.

calculated by the conductor-like polarized continuum model,[38] without further optimization of the geometry within the solvent medium.

The vertical energy of two triplet and two singlet excited states of the molecular and anionic reagent, in vacuo, was calculated using the time-dependent DFT method,[39] at the same level of theory, described above. The approximate structure of the S1 excited state of **10a** in vacuo was obtained after full geometry optimization by the CIS method,[30] using the 6-31G[40] basis set.

All calculations were performed by the Gaussian98 program package.[41]

Experimental Details. IR spectra were determined in Nujol mull. ^{1}H NMR spectra were recorded at 250 MHz using TMS as internal standard. Mass spectra were taken by using a GC chromatograph coupled with a MS detector (GC/MS). UV absorption spectra (Table 1) were recorded for **1a** in acetonitrile and cyclohexane for a comparison (Figure 1) with existing data in methanol[15] and for compounds **1b** (R = Me) and **10a,b** in methanol. Emission spectra were recorded in methanol. Compounds **1a,b**[14] and **10b**[20a] have been obtained as described previously. Compound **10a** was obtained in 8% yield by a procedure similar to that used for **10b**.[20a] Compound **10a** is a colorless oil: IR (Nujol) 3400, 3310, 3230, 3180 cm^{-1}; ^{1}H NMR (DMSO-d_6) δ 7.04 (s, exchangeable with D_2O); GC/MS *m*/*z* 153 (100) (M^+), 95 (27), 69 (90). Anal. Calcd for $C_3H_2F_3N_3O$: C, 23.54; H, 1.32; N, 27.45. Found: C, 23.60; H, 1.30; N, 27.50.

Acknowledgment. Financial support from the University of Palermo is gratefully acknowledged.

Supporting Information Available: Cartesian coordinates of compounds **10**−**21a,b** and **10**−**21a,b**$^-$ and of the transition states reported in Table 4. This material is available free of charge via the Internet at http://pubs.acs.org.

JO0525736

(38) Barone, V.; Cossi, M. *J. Phys. Chem. A* **1998**, *102*, 1995−2001.
(39) (a) Stratmann, R. E.; Scuseria, G. E.; Frisch, M. J. *J. Chem. Phys.* **1998**, *109*, 8218−8224. (b) Bauernschmitt, R.; Ahlrichs, R. *Chem. Phys. Lett.* **1996**, *256*, 454−464. (c) Casida, M. E.; Jamorski, C.; Casida, K. C.; Salahub, D. R. *J. Chem. Phys.* **1998**, *108*, 4439−4449.
(40) Hehre, W. J.; Ditchfield, R.; Pople, J. A. *J. Chem. Phys.* **1972**, *56*, 2257−2261.
(41) Frisch, M. J.; Trucks, G. W.; Schlegel, H. B.; Scuseria, G. E.; Robb, M. A.; Cheeseman, J. R.; Zakrzewski, V. G.; Montgomery, J. A., Jr.; Stratmann, R. E.; Burant, J. C.; Dapprich, S.; Millam, J. M.; Daniels, A. D.; Kudin, K. N.; Strain, M. C.; Farkas, O.; Tomasi, J.; Barone, V.; Cossi, M.; Cammi, R.; Mennucci, B.; Pomelli, C.; Adamo, C.; Clifford, S.; Ochterski, J.; Petersson, G. A.; Ayala, P. Y.; Cui, Q.; Morokuma, K.; Malick, D. K.; Rabuck, A. D.; Raghavachari, K.; Foresman, J. B.; Cioslowski, J.; Ortiz, J. V.; Baboul, A. G.; Stefanov, B. B.; Liu, G.; Liashenko, A.; Piskorz, P.; Komaromi, I.; Gomperts, R.; Martin, R. L.; Fox, D. J.; Keith, T.; Al-Laham, M. A.; Peng, C. Y.; Nanayakkara, A.; Challacombe, M.; Gill, P. M. W.; Johnson, B.; Chen, W.; Wong, M. W.; Andres, J. L.; Gonzalez, C.; Head-Gordon, M.; Replogle, E. S.; Pople, J. A. *Gaussian 98*, Revision A.8, Gaussian, Inc., Pittsburgh, PA, 1998.